

Symmetry Coordinates and Tentative Force Field Analysis of a $\text{PMo}_{12}\text{O}_{40}$ Model with the Keggin Structure

Lennart Lyhamn

Department of Inorganic Chemistry, The University of Umeå, S-901 87 Umeå, Sweden, and

S. J. Cyvin, B. N. Cyvin, and J. Brunvoll

Division of Physical Chemistry, The University of Trondheim,
N-7034 Trondheim-NTH, Norway

(Z. Naturforsch. 31 a, 1589–1600 [1976]; received October 3, 1976)

A complete vibrational analysis is performed for the 53 atomic $\text{PMo}_{12}\text{O}_{40}$ model of T_d symmetry. The symmetry coordinates are classified into those of (a) ligand vibrations, (b) framework-ligand couplings, (c) framework vibrations, and (d) interligand vibrations. Simple valence force fields are estimated, and the influence of inclusion of redundancies on the calculated frequencies and symmetry force constants is investigated. Comments are made on calculated symmetry force constant values up to 345 mdyne/Å. Vibrational frequencies are calculated for the Mo_3O_7 and Mo_3O_{13} units and for the $\text{PMo}_{12}\text{O}_{40}^{3-}$ complex ion. For the latter compound the calculated values are compared with experimental data from infrared and Raman spectra.

Introduction

Extensive spectroscopical studies have been made on inorganic complexes^{1–3}. A large experimental material is available from literature, as well as many normal-coordinate analyses.

Tetrahedral complexes with trigonal ligands have been studied in particular. Cyvin and Lyhamn⁴ have developed a theory for constructing symmetry coordinates suitable for the studies of kinematic effects^{5–8}. The theory was applied to the $\text{Ni}(\text{PF}_3)_4$ -type model⁹. Numerical computations are reported for the $\text{Ni}(\text{PF}_3)_4$ molecule¹⁰ and the $[\text{Zn}(\text{NH}_3)_4]^{2+}$ ion¹¹. In these works advantage was made of a classification of the vibrational modes into (a) framework vibrations, (b) framework-ligand couplings, and (c) ligand vibrations.

The present work was undertaken in connection with crystallographical and spectroscopical investigations of compounds with Keggin structures (see the subsequent sections). For such comparatively large compounds the assignments of infrared and Raman spectra are of course extremely difficult and should be supported by a normal coordinate analysis. However, the theoretical part of this analysis represents also a difficult problem. In the present work a successful analysis was achieved for a fifty-three atomic model applicable to the $\text{PMo}_{12}\text{O}_{40}^{3-}$ ion. It was possible to solve this problem by using

the above mentioned classification of the vibrational modes. This procedure was found to be useful in spite of the fact that the concept of ligands is introduced in an artificial way. The ligands are based on a mathematical viewpoint rather than a chemical one.

Theory

The $\text{PMo}_{12}\text{O}_{40}$ ion is assumed to have an over-all tetrahedral symmetry (T_d). Four Mo_3O_7 units with a trigonal (C_{3v}) symmetry are considered as the ligands. The model may be considered as an extension of the $\text{Ni}(\text{PF}_3)_4$ -type model⁹, but some new features occur in the present case. (1) The free ligands have genuine vibrations belonging to the a_2 species of C_{3v} . (2) The various ligands are linked together by bridging atoms giving rise to new types of vibrational modes here referred to as “interligand vibrations”. This type of modes is taken to include the so-called “interligand-ligand couplings”.

Numbering of Atoms

Table 1 gives a clue to the numbering of atoms in the $\text{PMo}_{12}\text{O}_{40}$ model. There are six sets of symmetrically equivalent atoms including four different types of oxygen. The atoms are numbered consecutively within each set. The sixteen atoms 1–16 are arranged around the central atom (here number 53) in the same way as in the $\text{Ni}(\text{PF}_3)_4$ -type model⁹.

Reprint requests to be sent to Prof. S. J. Cyvin, Division of Physical Chemistry, The University of Trondheim, N-7034 Trondheim-NTH, Norway.



Dieses Werk wurde im Jahr 2013 vom Verlag Zeitschrift für Naturforschung in Zusammenarbeit mit der Max-Planck-Gesellschaft zur Förderung der Wissenschaften e.V. digitalisiert und unter folgender Lizenz veröffentlicht: Creative Commons Namensnennung-Keine Bearbeitung 3.0 Deutschland Lizenz.

Zum 01.01.2015 ist eine Anpassung der Lizenzbedingungen (Entfall der Creative Commons Lizenzbedingung „Keine Bearbeitung“) beabsichtigt, um eine Nachnutzung auch im Rahmen zukünftiger wissenschaftlicher Nutzungsformen zu ermöglichen.

This work has been digitalized and published in 2013 by Verlag Zeitschrift für Naturforschung in cooperation with the Max Planck Society for the Advancement of Science under a Creative Commons Attribution-NoDerivs 3.0 Germany License.

On 01.01.2015 it is planned to change the License Conditions (the removal of the Creative Commons License condition “no derivative works”). This is to allow reuse in the area of future scientific usage.

Table 1. Numbering of atoms in the $\text{PMo}_{12}\text{O}_{40}$ model.

Ligand	A	B	C	D	
No.	1	2	3	4	O atoms arranged tetrahedrally
	5	8	11	14	Mo atoms
	6	9	12	15	
	7	10	13	16	
	17	20	23	26	O atoms in Mo_3O_3 rings
	18	21	24	27	
	19	22	25	28	
	29	32	35	38	free O atoms
	30	33	36	39	
	31	34	37	40	
	41	44	47	50	bridging O atoms in inter-ligand structures
	42	45	48	51	
	43	46	49	52	
	53				P atom

The $\text{PMo}_{12}\text{O}_{40}$ Model

The framework, PO_4 , is a well-known tetrahedral structure^{12, 13} shown in Figure 1. The atoms 1, 2, 3 and 4 are taken to belong to the ligands designated A, B, C and D, respectively. Figure 2 shows the framework-ligand coupling for the ligand A. A part of this structure is found in Fig. 3, where also a part of the ligand A itself is included. Here one should observe the almost planar four-membered ring, Mo_2O_2 . This structure resembles the molecular model of LiNaF_2 ¹⁴⁻¹⁶.

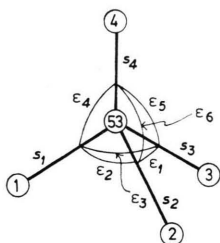
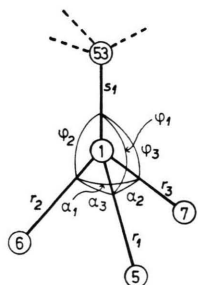
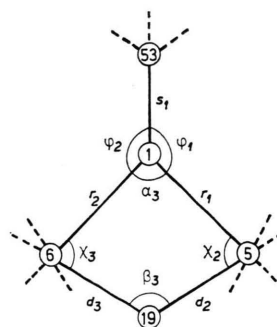
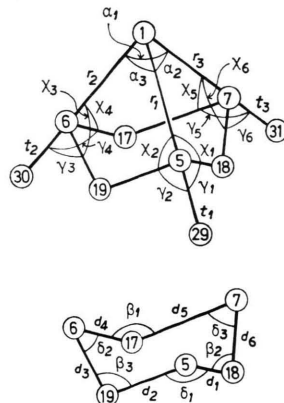
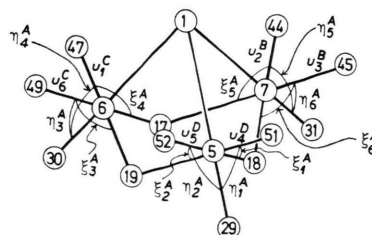
Fig. 1. Tetrahedral PO_4 (symmetry T_d) as a fragment of the $\text{PMo}_{12}\text{O}_{40}$ model.Fig. 2. Trigonal POMo_3 (symmetry C_{3v}) as a fragment of the $\text{PMo}_{12}\text{O}_{40}$ model.Fig. 3. POMo_2O as a fragment of the $\text{PMo}_{12}\text{O}_{40}$ model, showing the four-membered Mo_2O_2 ring.

Figure 4 shows one of the four Mo_3O_7 structures, viz. ligand A. The Mo_3O_3 puckered ring, which is a part of this ligand, is drawn separately. A similar six-membered ring structure is known from the molybdenum trioxide trimer, viz. Mo_3O_9 ¹⁷⁻¹⁹. The numbering of atoms in the corresponding ligands B, C and D is found in Table 1.

Figure 5 shows an extension of the ligand A into the Mo_3O_{13} structure obtained by including the adjacent bridging oxygen atoms. In this way a distorted octahedral arrangement emerges around each

Fig. 4. The Mo_3O_7 unit; symmetry C_{3v} . The six-membered Mo_3O_3 ring is also drawn separately.Fig. 5. The Mo_3O_{13} unit; symmetry C_{3v} .

molybdenum atom. One of these MoO_6 octahedra is shown in Fig. 6 and may be correlated to the corresponding well-known regular octahedral molecular model¹².

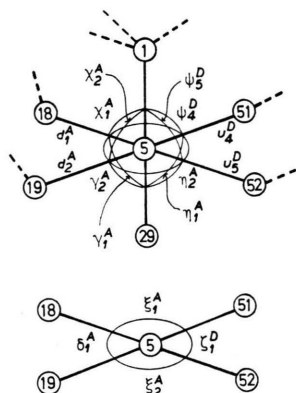


Fig. 6. The octahedral MoO_6 part of the $\text{PMo}_{12}\text{O}_{40}$ model. MoO_4 is also drawn separately.

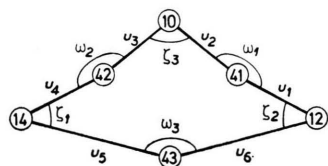


Fig. 7. The six-membered Mo_3O_3 ring (symmetry C_{3v}) made up from interligand bonds as a fragment of the $\text{PMo}_{12}\text{O}_{40}$ model.

Three bridging oxygen atoms form a puckered Mo_3O_3 ring together with the adjacent molybdenum atoms. One of these structures, here referred to as the interligand structures, is shown in Figure 7. This particular structure, which contains the oxygen atoms 41, 42 and 43 (cf. Table 1), is referred to as the interligand A and is found "opposite" to the ligand A when viewed along the bond 1–53. There are four of these structures in the whole complex, viz. A, B, C and D opposite to the ligands A, B, C and D, respectively. The numbering of oxygen atoms in the four interligand structures is found in Table 1.

Valence Coordinates

(a) Ligand vibrations. The stretching (r , d , t) and certain bending coordinates for the molecular vibrations of the Mo_3O_7 ligands are defined in Figure 4. We will use the notation r_1^A , r_2^A , ..., etc. for the ligand A (Fig. 4) and correspondingly r_1^B , r_2^B , ... for the ligand B, etc. The bendings α , β and χ are found in the almost planar Mo_2O_2 ring (see also

Figure 3). The β coordinates are also the MoOMo bendings of the puckered Mo_3O_3 ring (cf. the separate drawing of Fig. 4) with the δ coordinates as the OMoO bendings. The γ (OMoO) bendings involve the free oxygen atoms. We have also defined six p torsions (not indicated on the figures) for the puckered Mo_3O_3 ring in each ligand. The numbering follows the notation of the d stretchings, i.e. p_1^A (7-18-5-19), p_2^A (18-5-19-6), ..., etc.

(b) Framework-ligand couplings. The valence coordinates introduced for framework-ligand couplings are the φ bendings (cf. Figs. 2 and 3) and τ torsions. Figure 2 shows φ_1^A (5-1-53), φ_2^A and φ_3^A . Correspondingly one has φ_1^B , φ_2^B , ..., φ_3^D . The τ coordinates (not indicated on the figures) are the P–O bond torsions analogous with the τ 's of the $\text{Ni}(\text{PF}_3)_4$ model⁹. Thus we have τ_1^A (5-1-53-4), τ_2^A (6-1-53-3), τ_3^A (7-1-53-2), and correspondingly for τ_1^B , ..., τ_3^D .

(c) Framework vibrations. For the valence coordinates of the framework vibrations see Figure 1. They are the s stretchings and ε bendings.

(d) Interligand vibrations. The u stretchings and ω and ζ bendings of the interligand structure A are shown in Figure 7. In addition we have defined the q torsions as q_1^A (43-12-41-10), q_2^A (12-41-10-42), ..., q_6^A , q_1^B , ..., etc.

Under this category designated "interligand vibrations" we also include the coordinates for typical interligand-ligand coupling modes. They are the ξ , η and ψ bendings. The ξ (OMoO) and η ($\text{OMoO}_{\text{free}}$) coordinates associated with the ligand A are found in the Mo_3O_{13} structure deduced from this ligand; cf. Figure 5. Some of the ψ ($\text{O}_{\text{tetr.}}\text{MoO}$) coordinates are shown in Figure 6. Their notation follows the system used for the u stretchings.

Classification and Symmetry of the Normal Modes

The 24 normal modes of vibration for one Mo_3O_7 unit (Fig. 4) are distributed into the different species of the C_{3v} group according to

$$\Gamma(\text{Mo}_3\text{O}_7) = 6 a_1 + 2 a_2 + 8 e. \quad (1)$$

These modes give rise to $4 \cdot 24 = 96$ ligand vibrations of the whole complex. By means of the correlations between the symmetry species of the C_{3v} and T_d groups (cf. Table 2) one obtains

$$\Gamma(a) = 6 A_1 + 2 A_2 + 8 E + 10 F_1 + 14 F_2 \quad (2)$$

Table 2. Correlation table for the species of the symmetry group T_d with C_{3v} as a subgroup.

T_d :	A_1	A_2	E	F_1	F_2
C_{3v} :	a_1	a_2	e	$a_2 + e$	$a_1 + e$

Table 3. Classification of the normal modes. Correlations between the species of the groups C_{3v} and T_d are indicated.

Type	C_{3v}	T_d	Number of modes
(a) Ligand vibrations	4.6 a_1 4.2 a_2 4.8 e	6 $A_1 + 6 F_2$ 2 $A_2 + 2 F_1$ 8 $E + 8 F_1 + 8 F_2$	96
(b) Framework-ligand couplings		$A_2 + E + 2 F_1 + F_2$	12
(c) Framework vibrations		$A_1 + E + 2 F_2$	9
(d) Interligand vibrations	4.2 a_1 4. a_2 4.3 e	2 $A_1 + 2 F_2$ $A_2 + F_1$ 3 $E + 3 F_1 + 3 F_2$	36

for the distribution of the ligand vibration modes (a) into the species of the T_d group. Table 3 gives a more detailed account of the correlations; cf. also Reference⁴. The symmetrical structures of the framework-ligand couplings (b) and framework vibrations (c) are the same as the corresponding ones in the $\text{Ni}(\text{PF}_3)_4$ model⁴:

$$\Gamma(b) = A_2 + E + 2 F_1 + F_2, \quad (3)$$

$$\Gamma(c) = A_1 + E + 2 F_2. \quad (4)$$

For the interligand vibrations we must not reckon all the 12 modes of each Mo_3O_3 interligand structure because the molybdenum atoms are shared with the ligands. The proper number is 9, and these modes are distributed according to $2 a_1 + a_2 + 3 e$. They give rise to the $4 \cdot 9 = 36$ interligand vibrations (d) of the whole complex (cf. Table 3) with the symmetric structure

$$\Gamma(d) = 2 A_1 + A_2 + 3 E + 4 F_1 + 5 F_2. \quad (5)$$

The 153 normal modes of vibration of the whole complex are distributed according to

$$\Gamma = 9 A_1 + 4 A_2 + 13 E + 16 F_1 + 22 F_2 \quad (6)$$

which is the direct sum of Equations (2) – (5).

The 42 normal modes of vibration for one Mo_3O_{13} unit (Fig. 5) are distributed into the C_{3v} species according to:

$$\Gamma(\text{Mo}_3\text{O}_{13}) = 9 a_1 + 5 a_2 + 14 e.$$

Intermediate Symmetry Coordinates

In the attempts to construct a complete set of independent symmetry coordinates for the $\text{PMo}_{12}\text{O}_{40}$ ion we arrived at intermediate sets of C_{3v} symmetry coordinates for the ligands and interligand structures A, B, C and D. When properly combined these coordinates should constitute a part of the T_d symmetry coordinates for the whole complex. We also produced a set of symmetry coordinates for the Mo_3O_{13} unit by extending the set for a ligand (Mo_3O_7).

The bending and torsional coordinates were scaled by appropriate factors with the dimension of length. The capital letters S , R , D , T and U are used to designate the equilibrium distances corresponding to the stretchings denoted with the same small letters.

The Mo_3O_7 unit. The following set of symmetry coordinates was constructed for an isolated ligand (Figure 4).

$$S_1(a_1) = 3^{-\frac{1}{2}}(r_1 + r_2 + r_3),$$

$$S_2(a_1) = 6^{-\frac{1}{2}}(d_1 + d_2 + d_3 + d_4 + d_5 + d_6),$$

$$S_3(a_1) = 3^{-\frac{1}{2}}(t_1 + t_2 + t_3),$$

$$S_4(a_1) = 3^{-\frac{1}{2}}R(a_1 + a_2 + a_3),$$

$$S_5(a_1) = 3^{-\frac{1}{2}}D(\delta_1 + \delta_2 + \delta_3),$$

$$S_6(a_1) = (DT/6)^{\frac{1}{2}}(\gamma_1 + \gamma_2 + \gamma_3 + \gamma_4 + \gamma_5 + \gamma_6),$$

$$S_1(a_2) = 6^{-\frac{1}{2}}(d_1 - d_2 + d_3 - d_4 + d_5 - d_6),$$

$$S_2(a_2) = (DT/6)^{\frac{1}{2}}(\gamma_1 - \gamma_2 + \gamma_3 - \gamma_4 + \gamma_5 - \gamma_6),$$

$$S_{1a}(e) = 6^{-\frac{1}{2}}(2r_1 - r_2 - r_3),$$

$$S_{2a}(e) = 12^{-\frac{1}{2}}(2d_1 + 2d_2 - d_3 - d_4 - d_5 - d_6),$$

$$S_{3a}(e) = 6^{-\frac{1}{2}}(2t_1 - t_2 - t_3),$$

$$S_{4a}(e) = 6^{-\frac{1}{2}}R(2a_1 - a_2 - a_3),$$

$$S_{5a}(e) = 6^{-\frac{1}{2}}D(2\delta_1 - \delta_2 - \delta_3),$$

$$S_{6a}(e) = (DT/12)^{\frac{1}{2}}(2\gamma_1 - 2\gamma_2 - \gamma_3 - \gamma_4 - \gamma_5 - \gamma_6),$$

$$S_{7a}(e) = \frac{1}{2}(-d_3 + d_4 + d_5 - d_6),$$

$$S_{8a}(e) = \frac{1}{2}(DT)^{\frac{1}{2}}(-\gamma_3 + \gamma_4 + \gamma_5 - \gamma_6),$$

$$S_{1b}(e) = 2^{-\frac{1}{2}}(r_2 - r_3),$$

$$S_{2b}(e) = \frac{1}{2}(d_3 + d_4 - d_5 - d_6),$$

$$S_{3b}(e) = 2^{-\frac{1}{2}}(t_2 - t_3),$$

$$S_{4b}(e) = 2^{-\frac{1}{2}}R(a_2 - a_3),$$

$$S_{5b}(e) = 2^{-\frac{1}{2}}D(\delta_2 - \delta_3),$$

$$S_{6b}(e) = \frac{1}{2}(DT)^{\frac{1}{2}}(\gamma_3 + \gamma_4 - \gamma_5 - \gamma_6),$$

$$S_{7b}(e) = 12^{-\frac{1}{2}}(2d_1 - 2d_2 - d_3 + d_4 - d_5 + d_6),$$

$$S_{8b}(e) = (DT/12)^{\frac{1}{2}}(2\gamma_1 - 2\gamma_2 - \gamma_3 + \gamma_4 - \gamma_5 + \gamma_6).$$

This set of symmetry coordinates is complete although we have not used the valence coordinates of the types β , χ and p . The symmetry-adapted combinations of these coordinates might be included as redundancies. They are distributed according to

$$\Gamma\{\beta\} = a_1 + e, \quad \Gamma\{\chi\} = a_1 + a_2 + 2e \quad \text{and} \\ \Gamma\{p\} = a_1 + a_2 + 2e.$$

The Mo_3O_{13} unit. For the Mo_3O_{13} structure (Fig. 5) we have used the same expressions of symmetry coordinates as given above for Mo_3O_7 and augmented them in the following way in order to arrive at a complete set.

$$S_7(a_1) = 6^{-\frac{1}{2}}(u_1 + u_2 + u_3 + u_4 + u_5 + u_6), \\ S_8(a_1) = (D/U/6)^{\frac{1}{2}}(\xi_1 + \xi_2 + \xi_3 + \xi_4 + \xi_5 + \xi_6), \\ S_9(a_1) = (T/U/6)^{\frac{1}{2}}(\eta_1 + \eta_2 + \eta_3 + \eta_4 + \eta_5 + \eta_6).$$

It should be noticed that the u coordinates here refer to different interligand structures. When referring to the extended ligand A, u_1, \dots, u_6 are taken in the sense of $u_4^D, u_5^D, u_6^C, u_1^C, u_2^B, u_3^B$, respectively (cf. Figure 5). The appropriate combinations of u , ξ and η coordinates in species a_2 are added to the Mo_3O_7 coordinates correspondingly. In species e we have taken

$$S_{9a}(e) = 12^{-\frac{1}{2}}(2u_1 + 2u_2 - u_3 - u_4 - u_5 - u_6)$$

and the corresponding combinations of ξ and η coordinates for $S_{10a}(e)$ and $S_{11a}(e)$, respectively. Furthermore:

$$S_{12a}(e) = \frac{1}{2}(-u_3 + u_4 + u_5 - u_6)$$

and the corresponding combinations of ξ and η coordinates. Finally the b members of the e species were written up in an obvious way.

Again the complete set of symmetry coordinates may be supplemented with redundancies of the types β , χ and p , along with the additional types of ζ and ψ (cf. Figure 6).

Interligand vibrations. As intermediate symmetry coordinates for one of the interligand Mo_3O_3 structures (Fig. 7) we take the symmetry-adapted combinations of the six u coordinates and three ζ coordinates. They transform in the same way as d and r , respectively, i. e. $\Gamma\{u\} = a_1 + a_2 + 2e$ and $\Gamma\{\zeta\} = a_1 + e$.

Symmetry Coordinates for the Whole Complex

The intermediate symmetry coordinates were combined into final symmetry coordinates for the whole

Table 4. Types of symmetry coordinates for the whole complex.

Species	a		b		c		d			
	No.	Type	No.	Type	No.	Type	No.	Type		
A_1	1	$r(a_1)$	4	$\alpha(a_1)$		7	s	8	$u(a_1)$	
	2	$d(a_1)$	5	$\delta(a_1)$				9	$\zeta(a_1)$	
	3	$t(a_1)$	6	$\gamma(a_1)$						
A_2	1	$d(a_2)$		3	$\tau(a_2)$			4	$u(a_2)$	
	2	$\gamma(a_2)$								
E	1	$r(e)$	5	$\delta(e)$	9	$\varphi(e)$	10	ε	11	$u(e)$
	2	$d(e)$	6	$\gamma(e)$					12	$\zeta(e)$
	3	$t(e)$	7	$d(e)$					13	$u(e)$
	4	$\alpha(e)$	8	$\gamma(e)$						
F_1	1	$d(a_2)$	6	$\alpha(e)$	11	$\varphi(e)$			13	$u(a_2)$
	2	$\gamma(a_2)$	7	$\delta(e)$	12	$\tau(a_2)$			14	$u(e)$
	3	$r(e)$	8	$\gamma(e)$					15	$\zeta(e)$
	4	$d(e)$	9	$d(e)$					16	$u(e)$
	5	$t(e)$	10	$\gamma(e)$						
F_2	1	$r(a_1)$	8	$d(e)$	15	$\varphi(e)$	16	s	18	$u(a_1)$
	2	$d(a_1)$	9	$t(e)$			17	ε	19	$\zeta(a_1)$
	3	$t(a_1)$	10	$\alpha(e)$					20	$u(e)$
	4	$\alpha(a_1)$	11	$\delta(e)$					21	$\zeta(e)$
	5	$\delta(a_1)$	12	$\gamma(e)$					22	$u(e)$
	6	$\gamma(a_1)$	13	$d(e)$						
	7	$r(e)$	14	$\gamma(e)$						

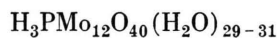
a Ligand vibrations. b Framework-ligand couplings.

c Framework vibrations. d Interligand vibrations.

complex by means of the general expressions given previously⁴ and supplemented recently²⁰. Table 4 gives a survey of the types of symmetry coordinates in terms of the valence coordinates used to develop them. The table includes the species of C_{3v} in parentheses. (a) The symmetry coordinates of ligand vibrations are constructed from those of the free ligands (Mo_3O_7 ; see above) according to the general formulas given in Ref. 4 for A_1 , E , F_2 and a part of F_1 , and in Ref. 20 for A_2 and the rest of F_1 . (b) The coordinates of framework-ligand couplings from the φ coordinates are obtained by analogy with the corresponding r -type coordinates. As for the τ coordinates we have the normalized sum of the twelve τ 's in A_2 , while the F_1 coordinates are analogous to those specified for the $\text{Ni}(\text{PF}_3)_4$ model²⁰. (c) The framework vibrations are analogous to those of the $\text{Ni}(\text{PF}_3)_4$ model⁹. (d) The coordinates of interligand vibrations are obtained in the same way as those of the ligand vibrations by means of the general formulas^{4, 20}.

Structural Parameters

A complete structure determination of



has been made by Strandberg²¹. The structure of the analogous $\text{H}_3\text{PW}_{12}\text{O}_{40}$ compound was predicted by Keggin already in 1934²², and geometrical arrangements of this type (cf. Fig. 8) are often called Keggin structures. Another structure determination of a $\text{Na}_3\text{H}_6\text{PMo}_9\text{O}_{34}(\text{H}_2\text{O})_x$ phase with an incomplete Keggin structure is due to Strandberg²³.

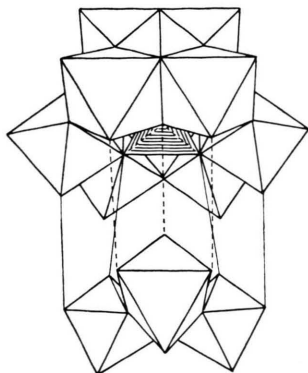


Fig. 8. The coupling of the twelve MoO_6 octahedra and the PO_4 tetrahedron in the $\text{PMo}_{12}\text{O}_{40}$ model shown with idealized polyhedra; cf. also Reference²¹.

In the present analysis an idealized structure being exactly tetrahedral (symmetry T_d) was assumed for the $\text{PMo}_{12}\text{O}_{40}^{3-}$ ion. The cartesian coordinates for the 53 atoms were deduced on the basis of single crystal data²¹; the corresponding bond and interbond angle values are shown in Table 5. Most of the cartesian coordinate values are

Table 5. Structural parameters in tetrahedral $\text{PMo}_{12}\text{O}_{40}^{3-}$.

Bond or angle	Å or degrees	Atom numbers	Reference to Fig. No.
P—O	1.542	1-53	1, 2, 3
Mo—O _{tetr.}	2.433	1-5	2, 3, 4
Mo—O	1.922	5-18 (19)	3, 4, 6
Mo—O _{free}	1.677	5-29	4
Mo—O _{br.}	1.912	12-41	7
OPO	109.47	1-53-4	1
	(tetrahedral)		
POMo	125.80	53-1-5	2, 3
MoO _{tetr.} Mo	89.24	5-1-6	2, 3, 4
MoOMo	125.52	5-19-6	3, 4
O _{tetr.} MoO	72.59	1-5-18 (19)	3, 4, 6
OMoO	86.92	18-5-19	4, 6
OMoO _{free}	100.86	18-5-29	4, 6
OMoO _{br.}	88.51	18-5-51	5, 6
O _{free} MoO _{br.}	103.04	29-5-51	5, 6
O _{br.} MoO _{br.}	86.24	42-14-43	7
MoO _{br.} Mo	151.07	10-42-14	7

very close to the experimental data, although not within the estimated standard deviations. The coordinates of the interligand bridging O atoms got the greatest deviations, resulting in errors of about 0.05 Å in some of the bond lengths.

Force Field Calculations

It is of interest to investigate various approximate force fields for the $\text{PMo}_{12}\text{O}_{40}^{3-}$ ion to develop force constants, which it should be possible to transfer to related structures. We are also interested in the comparisons with calculated frequencies for Mo_3O_7 and Mo_3O_{13} treated as isolated units.

Approximate Force Constants

In all the present calculations a diagonal valence force constant matrix was assumed, but allowance was made for redundancies. Diagonal force constant matrices based on coordinates with redundancies usually give rise to off-diagonal terms when converted to a standard F matrix based on independent coordinates.

The Mo—O stretching force constants were produced by means of their empirical correlations with bond lengths according to Cotton et al.²⁴. The bending and torsional force constants are more or less arbitrary values, estimated with the aid of unpublished calculations on $(\text{MoO}_3)_3$ as far as the orders of magnitude are concerned. Some more extensive calculations are reported for the related compound $(\text{WO}_3)_3$ ²⁵. Altogether the following numerical values (all in mdyne/Å) were estimated.

$$f_s(\text{P—O}) = 4.5,$$

$$f_r(\text{Mo—O}_{\text{tetr.}}) = 0.8, \quad f_d = f_u = 4.0.$$

for the Mo—O stretchings in four-membered or six-membered rings.

$$f_t = 7.4$$

for the free Mo—O bonds.

$$f_e(\text{OPO}) = f_\varphi(\text{POMo}) = 0.40, \quad f_a(\text{MoOMo}) = 0.45.$$

For OMoO (χ) and MoOMo (β) bendings in the four-membered ring, the latter also taking part in a six-membered ring:

$$f_z = f_\beta = 0.35.$$

Octahedral OMoO bendings involving bridging O atoms only:

$$f_\delta = f_\zeta = f_\psi = f_\xi = 0.30.$$

Octahedral OMoO bendings involving a free oxygen atom:

$$f_\gamma = f_\eta = 0.25.$$

MoOMo bendings for the bridging part of a six-membered ring:

$$f_\omega = 0.25.$$

Torsions:

$$f_p = f_q = f_\tau = 0.02.$$

The Mo_3O_7 Unit

Calculated frequencies from three runs are given in Table 6 in order to show the importance of including redundancies. Computations were performed

Table 6. Calculated frequencies (cm^{-1}) for the Mo_3O_7 unit.

Species	Approximate description	a	b	c
a_1	t	959	963	963
	d	565	687	689
	$\alpha + r$	522	585	586
	δ	365	372	396
	$r + d + \alpha$	80	269	277
	γ	203	166	168
a_2	d	862	874	875
	γ	203	203	203
e	t	961	964	964
	d	867	880	881
	d'	545	674	677
	$\alpha + r$	375	452	452
	mixed	84	257	259
	$\gamma (+\delta)$	224	224	237
	$\delta + \gamma'$	192	176	190
		174	149	160

a Without redundancies. b Redundancies without torsions.
c Redundancies including torsions.

ed (a) without redundancies, corresponding to a diagonal F matrix in terms of the independent symmetry coordinates given above, (b) with additional bendings (β and χ types) included as redundancies, and (c) with all of the relevant coordinate types, including p torsions. Rather drastic frequency shifts are found, especially from Set a to Set b (Table 6). We believe that Set c is the best one of these three calculations. The approximate description of normal modes included in Table 6 are deduced with the aid of calculated potential energy distributions. They should be considered as suggestions only, especially because the terms undergo great changes through the three sets of calculations. It seems to be of interest to show some of the derived symmetry force

Table 7. Symmetry force constants ($\text{mdyne}/\text{\AA}$) for the a_1 species of Mo_3O_7 from two calculations.

(a) without redundancies. Diagonal matrix:					
0.800	4.000	7.400	0.450	0.300	0.250
(c) with redundancies including torsions *					
r	d	t	α	δ	γ
6.514					
-5.114	8.577				
0.000	0.000	7.400			
3.425	-3.066	0.000	2.585		
0.155	-0.139	0.000	0.086	0.358	
0.000	0.000	0.000	0.000	0.000	0.250

* Only the whole block of the F matrix has physical meaning with reference to the particular set of symmetry coordinates. The warning in text concerning interpretations of the individual force constants should be noticed.

constants. Table 7 includes the F matrix block of species a_1 from the calculations of Set c. It is instructive to compare the values on the main diagonal with those from the calculation (a) without redundancies. All of them except f_t and f_γ for the vibrations involving free oxygen atoms are found to

Table 8. Calculated frequencies (cm^{-1}) for the Mo_3O_{13} unit.

Species	Approximate description	a	b	c
a_1	t	961	967	967
	$u + d$	727	738	745
	$\alpha + d + r$	545	681	683
	$\delta + \xi$	522	605	609
	η	444	448	515
	$\eta + \delta + \xi$	271	369	369
	$\eta + \delta + \xi$	128	302	309
	γ (mixed)	215	239	240
	$r + \alpha + \gamma$	49	166	173
a_2	d	873	885	887
	u	692	693	693
	$\eta + \gamma$	300	311	311
	$\xi + \gamma$	213	258	258
	$\gamma + \xi$	96	161	161
e	t	963	967	968
	d	877	891	892
	u'	724	734	735
	u	696	698	699
	d'	528	636	640
	$\alpha + r$	376	505	505
	$\xi + \xi'$	355	367	409
	η	300	341	342
	$\xi + \xi'$	191	318	324
	η'	263	300	301
	γ	179	247	247
		123	237	239
	mixed	102	174	175
		45	98	125

a-c See footnotes to Table 6.

Table 9. Symmetry force constants (mdyne/Å) for the a_1 species of Mo_3O_{13} from two calculations.

(a) without redundancies. Diagonal matrix:								
0.800	4.000	7.400	0.450	0.300	0.250	4.000	0.300	0.250
(c) with redundancies including torsions *								
r	d	t	α	δ	γ	u	ξ	η
8.841								
-7.197	10.442							
0.000	0.000	7.400						
5.100	-4.565	0.000	3.808					
0.624	-0.558	0.000	0.367	0.812				
-0.904	0.809	0.000	-0.682	0.108	0.774			
0.000	0.000	0.000	0.000	0.000	0.000	4.000		
0.101	-0.091	0.000	0.076	0.444	0.223	0.000	0.927	
-0.908	0.813	0.000	-0.685	0.109	0.526	0.000	0.224	0.787

* See footnote to Table 7.

undergo drastic changes. They all increase, as is necessary to compensate for the omission of redundancies in the set of symmetry coordinates. There are also found substantial off-diagonal terms in the F matrix block, which hardly could be estimated in advance.

The Mo_3O_{13} Unit

Calculated frequencies for the Mo_3O_{13} unit were produced in the same way as described above for Mo_3O_7 . Table 8 shows the results Set a (calculated without redundancies), Set b (with bendings as redundancies) and Set c (with all redundancies including torsions). Table 9 shows the symmetry F matrix blocks of species a_1 from Sets a and c. It is also interesting to observe the great differences in corresponding force constant values from Set c of Mo_3O_7 (Table 7) and Mo_3O_{13} (Table 9).

The Whole Complex

It was decided to perform the most detailed analysis of species A_1 for the $\text{PMo}_{12}\text{O}_{40}^{3-}$ complex. Table 10 shows the calculated frequencies with simple force fields based on the coordinates (a) without redundancies, (b) with bendings for the ligand vibrations (β and χ types) as redundancies, (c) with all bendings (including those of the framework-ligand couplings and interligand vibrations) as redundancies, and (d) with all redundancies, including torsions. We find extremely large differences in the calculated frequencies from one set to another, thus emphasizing the importance of including redundancies in the analysis. The force constants from the calculations a and d are shown in

Table 10. Calculated A_1 frequencies (cm^{-1}) for $\text{PMo}_{12}\text{O}_{40}^{3-}$.

a	b	c	d
961	964	978	979
872	908	958	958
570	680	685	688
414	432	580	582
377	391	459	546
243	293	429	452
204	221	288	309
78	157	238	240
30	33	192	206

a Without redundancies.

b With bending redundancies for ligand vibrations.

c With all bending redundancies.

d With all redundancies including torsions.

Table 11. The inclusion of redundancies in Set d is seen to have a tremendous effect on the F matrix; force constant values up to 345 mdyne/Å have hardly been published before! Nevertheless we claim that these seemingly pathological values are introduced in a natural way through the mathematical conversion of a reasonable diagonal force constant matrix. Anyhow the case seems to deserve a closer inspection in order to convince all readers that we have not committed bad miscalculations. The mathematical reason why the calculated frequencies come out with normal values is found in the numerical form of the inverse G matrix, which also has elements of abnormally large magnitudes. The A_1 block of G^{-1} is shown in Table 12. This means that the G matrix tends to be singular. We feared that almost singularity of the G matrix might cause numerical instability in the solution of the secular equation. However, a backward calculation with the aid of the eigenvector matrix L (with elements of normal mag-

Table 11. Symmetry force constants (mdyne/Å) for the A_1 species of $\text{PMo}_{12}\text{O}_{40}^{3-}$ from two calculations.

(a) without redundancies. Diagonal matrix:								
0.800	4.000	7.400	0.450	0.300	0.250	4.500	4.000	0.300
(d) with redundancies including torsions *								
r	d	t	α	δ	γ	s	u	ζ
21.50								
-7.92	9.67							
0.00	0.00	7.400						
-24.06	0.12	0.000	59.95					
0.76	-0.37	0.000	-0.60	0.529				
-1.21	0.47	0.000	1.37	-0.028	0.498			
68.84	-9.20	0.000	-138.97	1.990	-3.961	344.7		
-33.33	4.46	0.000	67.28	-0.964	1.918	-164.7	83.73	
5.45	-0.81	0.000	-10.70	0.298	-0.275	26.4	-12.77	2.707

* See footnote to Table 7.

Table 12. Inverse G matrix elements (amu) for the A_1 species of $\text{PMo}_{12}\text{O}_{40}^{3-}$.

r	d	t	α	δ	γ	s	u	ζ
195.0								
-70.6	91.22							
15.8	0.00	16.00						
-71.6	-39.67	-1.82	513.6					
7.3	-7.06	-0.00	7.2	4.679				
-26.6	25.96	-0.00	-4.4	-1.528	13.70			
340.8	7.83	19.63	-1099.6	-7.011	-18.10	2560		
-109.0	-0.00	-0.00	500.2	0.000	0.00	-1111	575.9	
18.3	0.00	0.00	-83.9	-0.000	-0.00	186	-92.0	18.89

nitudes) reproduced the original F and G matrices with almost exactness, and thus convinced us of the correctness of the analysis. It is also supported by the compliance matrix calculations reported in the subsequent section.

The effects of kinematic coupling may be studied by comparing the frequencies of Table 10 with those of the Mo_3O_7 unit (Table 6). It is relevant to compare columns a in both tables. Set b of Table 6 may be compared to columns b and c of Table 10, and finally the calculations c for Mo_3O_7 (Table 6) should be correlated to those of d from Table 10. A detailed interpretation of the frequency shifts, however, is hardly possible because the ligand vibration modes in the complex are highly mixed with the other modes. Nevertheless a correlation between the frequencies of $\text{PMo}_{12}\text{O}_{40}^{3-}$ with those of Mo_3O_7 as well as Mo_3O_{13} was attempted, using the numerical correspondence between the frequency values.

Table 13 shows the final values of calculated frequencies for all species of $\text{PMo}_{12}\text{O}_{40}^{3-}$. This set is based on the analysis including all the redundancies specified above. The values are tentatively correlated to those of Mo_3O_7 and Mo_3O_{13} .

Compliants

Among the given symmetry force constants (Tables 7, 9 and especially 11) many abnormally high values are found. It is clear that it would be meaningless to interpret them as stretchings, bendings, etc., according to the corresponding coordinates. Compliance constants on the other hand possess the certain type of invariance properties which always make it feasible to associate them with the appropriate coordinate pairs. We produced the compliance matrix for species A_1 of $\text{PMo}_{12}\text{O}_{40}^{3-}$ by inversion of the F matrix block given in Table 11. It is a pleasing fact to observe that all the compliants came out with normal values for such constants (see Table 14). They are seen to be comparable with those of species a_1 for Mo_3O_7 also included in Table 14. Most of the principal compliants (i. e. those on the main diagonal) are seen to have similar magnitudes. Only those of the α and γ type coordinates are found to undergo substantial shifts. Considerations of this type are perfectly meaningful because of the possibility to interpret the compliants as physical constants associated with the different coordi-

Table 13. Calculated frequencies (cm^{-1}) for $\text{PMo}_{12}\text{O}_{40}^{3-}$ correlated to those of Mo_3O_7 and Mo_3O_{13} .

correlated to those of Mo ₃ O ₇ and Mo ₃ O ₁₃ .							
Species of PMo ₁₂ O ₄₀	PMo ₁₂ O ₄₀ (Td)	Mo ₃ O ₇ (C _{3v})	Mo ₃ O ₁₃ (C _{3v})	Species of PMo ₁₂ O ₄₀	PMo ₁₂ O ₄₀ (Td)	Mo ₃ O ₇ (C _{3v})	Mo ₃ O ₁₃ (C _{3v})
A ₁ :	979			F ₂ :	653		640 (e)
					537	677 (e)	505 (e)
	958	963 (a ₁)	967 (a ₁)		445	452 (e)	409 (e)
			745 (a ₁)		355		342 (e)
	688	689 (a ₁)	683 (a ₁)				324 (e)
	582	586 (a ₁)	609 (a ₁)		312		311 (a ₂)
	546		515 (a ₁)		281		301 (e)
	452	396 (a ₁)	369 (a ₁)		268	259 (e)	258 (a ₂)
	309	277 (a ₁)	309 (a ₁)				247 (e)
	240		240 (a ₁)			237 (e)	239 (e)
206	168 (a ₁)	173 (a ₁)	222		203 (a ₂)	161 (a ₂)	
A ₂ :	948				196	190 (e)	175 (e)
	857	875 (a ₂)	887 (a ₂)		137	160 (e)	125 (e)
			693 (a ₂)				
	289		311 (a ₂)				
E:			258 (a ₂)		975	964 (e)	968 (e)
	120	203 (a ₂)	161 (a ₂)		970	963 (a ₁)	967 (a ₁)
	974				941		
	945	964 (e)	968 (e)		885	881 (e)	892 (e)
	883	881 (e)	892 (e)		799		745 (a ₁)
	768		735 (e)				735 (e)
			699 (e)		688	689 (a ₁)	699 (e)
	675	677 (e)	640 (e)		678	677 (e)	683 (a ₁)
	547	452 (e)	505 (e)		571	586 (a ₁)	640 (e)
	463		409 (e)		549		609 (a ₁)
F ₁ :			342 (e)		528	452 (e)	515 (a ₁)
	316		324 (e)		469		505 (e)
	296		301 (e)		466		
	249	259 (e)	247 (e)		422		409 (e)
	205	237 (e)	239 (e)		358	396 (a ₁)	369 (a ₁)
	174	190 (e)	175 (e)	327		342 (e)	
	154	160 (e)	125 (e)			324 (e)	
	973			284	277 (a ₁)	309 (a ₁)	
	955	964 (e)	968 (e)			301 (e)	
	939	881 (e)	892 (e)	269	259 (e)	247 (e)	
876	875 (a ₂)	887 (a ₂)			240 (a ₁)		
862		735 (e)	233	237 (e)	239 (e)		
		699 (e)	219	190 (e)	175 (e)		
		693 (a ₂)	197	168 (a ₁)	173 (a ₁)		
			170	160 (e)	125 (e)		

Table 14. Compliants ($\text{\AA}/\text{mdyne}$) for species a_1 of Mo_3O_7 (Set c) and species A_1 of $\text{PMo}_{12}\text{O}_{40}^{3-}$ (Set d).

Mo_3O_7	r	d	t	α	δ	γ			
	0.572								
	0.121	0.228							
	0.000	0.000	0.135						
	-0.612	0.110	0.000	1.328					
	-0.054	0.010	0.000	-0.011	2.823				
	0.000	0.000	0.000	0.000	0.000	4.000			
$\text{PMo}_{12}\text{O}_{40}^{3-}$	r	d	t	α	δ	γ	s	u	ζ
	0.354								
	0.140	0.226							
	0.000	0.000	0.135						
	-0.213	0.074	0.000	0.555					
	-0.057	0.012	0.000	-0.053	2.125				
	0.106	-0.016	0.000	0.024	-0.039	2.340			
	-0.116	0.006	0.000	0.207	0.009	0.019	0.136		
	0.063	-0.003	0.000	-0.113	-0.005	-0.010	0.047	0.224	
	-0.070	0.004	0.000	0.108	-0.437	-0.118	-0.049	0.027	1.584

Table 15. Calculated and observed frequencies (cm^{-1}) for $\text{PMo}_{12}\text{O}_{40}^{3-}$.

Calculated				Observed	
A_1 (Ra)	E (Ra)	F_2 (IR + Ra)	Tentative description	Infrared	Raman
		1107	P—O stretch	1070	1090 (vw)
980			P—O stretch	990 ^a	996 (vs)
	974	975	Mo—O _t stretch (<i>e</i>)	965	
958		970	Mo—O _t stretch (a_1)		977 (s)
	945	941	Mo—O (P) stretch (<i>e</i>)	898 ^a	895
	883	885		870	825 (?)
		799		790	
	768	}	Mo—O _b stretch		
688			Mo—O (P) stretch (a_1)		718
	675	688			710
582		678			602 (s)
		571	bridge stretching and deformations	598	
546	547	549		560 ^a	580 ^b
		528		500	495 (w)
		469		465 ^a	463
	463	466		460	463
452					missing?
		422		410	406 ^b
		358		380	375 (doublet)
		327		340	340 (?)
	316				
309	296				missing?
		284		282	
		269		265	
	249				
240					247 (s)
		233		220	220
		219		220	} (broad)
206	205				
		197		—	} (doublet)
	174	170		—	
	154				110 (doublet)
					75

^a From Lange et al. ²⁶; all other infrared frequencies from Thouvenot et al. ²⁷.^b From Thouvenot et al. ²⁷; all other Raman frequencies are taken from Ref. ²⁸.

nates. Here we have given the compliants for two selected blocks only, although many more of them were computed. A more extensive report seems not to be warranted at this stage of the work.

Comparison with Observed Frequencies

It is clear that the present approximate analysis cannot predict the fundamental frequencies with any large degree of accuracy. Nevertheless we find the calculated frequencies to be distributed in the correct ranges of experimental frequencies when compared with the measurements available so

far ^{26–28}. Table 15 shows the spectroscopically active frequencies of the present calculations tentatively correlated with the experimental data. Apart from the fact that the general picture is correctly reproduced by the calculations one also finds remarkably many instances of quantitative agreements. The table includes a suggestion to a partial approximate description of the normal modes.

Acknowledgement

Financial support to BNC from The Norwegian Research Council for Science and the Humanities is gratefully acknowledged.

¹ K. Nakamoto, *Infrared Spectra of Inorganic and Coordination Compounds*, 2nd Edition, Wiley-Interscience, New York 1970.

² H. Siebert, *Anwendungen der Schwingungsspektroskopie in der anorganischen Chemie*, Springer-Verlag, Berlin 1966.

- ³ D. M. Adams, *Metal-Ligand and Related Vibrations*, Arnold, London 1967.
- ⁴ S. J. Cyvin and L. Lyhamn, *J. Mol. Struct.* **25**, 151 [1975]; erratum: *ibid.* **28**, 452 [1975].
- ⁵ P. Gans, *Vibrating Molecules*, Chapman and Hall, London 1971.
- ⁶ L. Schäfer, S. J. Cyvin, and J. Brunvoll, *Tetrahedron* **27**, 6177 [1971].
- ⁷ S. J. Cyvin, *Rev. Chim. Minerale* **11**, 1 [1974].
- ⁸ S. J. Cyvin, *Spectrochim. Acta* **30 A**, 263 [1974].
- ⁹ R. Andreassen, S. J. Cyvin, and L. Lyhamn, *J. Mol. Struct.* **25**, 155 [1975].
- ¹⁰ S. J. Cyvin, *Z. Anorg. Allgem. Chem.* **403**, 193 [1974].
- ¹¹ S. J. Cyvin, B. N. Cyvin, R. Andreassen, and A. Müller, *J. Mol. Struct.* **25**, 141 [1975].
- ¹² S. J. Cyvin, *Molecular Vibrations and Mean Square Amplitudes*, Universitetsforlaget, Oslo, and Elsevier, Amsterdam 1968.
- ¹³ S. J. Cyvin, B. N. Cyvin, I. Elvebredd, G. Hagen, and J. Brunvoll, *Kgl. Norske Videnskab. Selskabs Skrifter*, **1972**, No. 22.
- ¹⁴ S. J. Cyvin, B. N. Cyvin, and A. Snelson, *J. Phys. Chem.* **74**, 4338 [1970].
- ¹⁵ B. N. Cyvin and S. J. Cyvin, in S. J. Cyvin (ed.), *Molecular Structures and Vibrations*, Elsevier, Amsterdam 1972, p. 243.
- ¹⁶ A. Snelson, B. N. Cyvin, and S. J. Cyvin, in S. J. Cyvin (ed.), *Molecular Structures and Vibrations*, Elsevier, Amsterdam 1972, p. 246.
- ¹⁷ J. Berkowitz, M. G. Inghram, and W. Chupka, *J. Chem. Phys.* **26**, 842 [1957].
- ¹⁸ P. A. Perov, V. N. Novikov, and A. A. Maltsev, *Vestn. Moskov. Univ. Khimiya* **13**, 89 [1972].
- ¹⁹ N. M. Egorova and N. G. Rambidi, in S. J. Cyvin (ed.), *Molecular Structures and Vibrations*, Elsevier, Amsterdam 1972, p. 212.
- ²⁰ S. J. Cyvin, *J. Mol. Struct.* **30**, 311 [1976].
- ²¹ R. Strandberg, *Acta Chem. Scand. A* **29**, 359 [1975].
- ²² J. F. Keggin, *Proc. Roy. Soc. London* **144**, 75 [1934].
- ²³ R. Strandberg, *Acta Chem. Scand. A* **28**, 217 [1974].
- ²⁴ F. A. Cotton and R. M. Wing, *Inorg. Chem.* **4**, 867 [1965].
- ²⁵ B. N. Cyvin, M. Hargittai, S. J. Cyvin, and I. Hargittai, *Acta Chim. Hung.* **84**, 55 [1975].
- ²⁶ G. Lange, H. Hahn, and K. Dehnicke, *Z. Naturforsch.* **24b**, 1498 [1969].
- ²⁷ R. Thouvenot, C. Rocchiccioli-Deltcheff, and P. Souchay, *C. R. Acad. Sci. Paris Ser. C* **1974**, 455.
- ²⁸ L. Lyhamn, L. Pettersson, and N. Ingri, to be published.